Characterization of two new high-grade B-cell lymphoma cell lines with MYC and BCL2 rearrangements that are suitable for in vitro drug sensitivity studies

Journal:	*Leukemia and Lymphoma*
Manuscript ID	GLAL-2018-0194.R1
Manuscript Type:	Original Article - Research
Date Submitted by the Author:	n/a
Complete List of Authors:	Dheur, Marie-Sophie; Institut de Duve, Cellular Genetics Unit Antoine-Poirel, Hélène; Cliniques universitaires Saint-Luc, Centre de Génétique Humaine Ameye, Geneviève; Cliniques universitaires Saint-Luc, Centre de Génétique Humaine Tilman, Gaëlle; Cliniques universitaires Saint-Luc, Centre de Génétique Humaine Saussoy, Pascale; Cliniques universitaires Saint-Luc, Department of Clinical Biology Defour, Jean-Philippe; Cliniques universitaires Saint-Luc, Department of Clinical Biology Camboni, Alessandra; Cliniques universitaires Saint-Luc, Department of Pathology; Cliniques universitaires Saint-Luc, Department of Hematology Van Den Neste, Eric; Cliniques universitaires Saint-Luc, Hematology Coulie, Pierre; Institut de Duve van Baren, Nicolas; Institut de Duve,
Keywords:	High-grade double-hit lymphoma, MYC, BCL2, Cell lines

Characterization of two new high-grade B-cell lymphoma cell lines with *MYC* and *BCL2* rearrangements that are suitable for *in vitro* drug sensitivity studies

Marie-Sophie Dheur[1], Hélène A. Poirel[2+], Geneviève Ameye[2*], Gaëlle Tilman[2], Pascale Saussoy[3], Jean-Philippe Defour[3], Alessandra Camboni[4,5], Eric Van Den Neste[5], Pierre G. Coulie[1], Nicolas van Baren[1]

[1] *Cellular Genetics Unit, de Duve Institute, Université catholique de Louvain, Brussels, Belgium ; Avenue Hippocrate, 75 – B1.74.04 – B-1200 Brussels, Belgium*

[2] *Centre de Génétique Humaine, Cliniques universitaires Saint-Luc, Université catholique de Louvain, Avenue Hippocrate, 10 – B-1200 Brussels, Belgium*

[3] *Department of Clinical Biology, Cliniques universitaires Saint-Luc, Université catholique de Louvain, Avenue Hippocrate, 10 – B-1200 Brussels, Belgium*

[4] *Department of Pathology, Cliniques universitaires Saint-Luc, Université catholique de Louvain, Tour Franklin, Avenue Mounier – B-1200 Brussels, Belgium*

[5] *Department of Hematology, Cliniques universitaires Saint-Luc, Université catholique de Louvain, Avenue Hippocrate, 10 – B-1200 Brussels, Belgium*

[+] *Currently Belgian Cancer Registry, Brussels, Belgium*

* *Currently Centrum Menselijke Erfelijkheid, Universitair Ziekenhuis, Leuven, Belgium*

E-mail addresses and telephone numbers for all authors:

marie-sophie.dheur@uclouvain.be, +32 2 764 75 08

helene.antoine-poirel@gmx.com, +32 2 21 08 50

genevieve.ameye@uzleuven.be, +32 16 34 51 67
gaelle.tilman@uclouvain.be, +32 2 764 67 76
pascale.saussoy@uclouvain.be, +32 2 764 67 80
jean-philippe.defour@uclouvain.be, +32 2 764 68 14
alessandra.camboni@uclouvain.be, +32 2 764 67 58
eric.vandenneste@uclouvain.be, +32 2 764 18 00
pierre.coulie@uclouvain.be, +32 2 764 75 81
nicolas.vanbaren@uclouvain.be, +32 2 764 75 08

Correspondence: nicolas.vanbaren@uclouvain.be

Word count: 3271 words (abstract included)

Characterization of two new high-grade B-cell lymphoma cell lines with *MYC* and *BCL2* rearrangements that are suitable for *in vitro* drug sensitivity studies

High-grade B-cell lymphomas with *MYC* and *BCL2* or *BCL6* rearrangements are highly aggressive B-cell lymphomas called double-hit lymphomas (HGBL-DH). They are particularly refractory to standard treatments and carry a poor prognosis. Fragments of resected tumoural lymph nodes from two HGBL-DH patients were put in culture. Continuously proliferating cells were characterized and compared with the original tumours. In both cases, the proliferating cells and the tumour displayed *MYC* and *BCL2* rearrangements. Both cell lines (called LB5848-LYMP and LB5871-LYMP) presented a high proliferation rate and were maintained in culture for more than one year. Upon injection in immunodeficient mice, LB5848-LYMP gave rise to lymphoid tumours. *In vitro* treatment of these cell lines with a BCL2-inhibitory drug (ABT-199) selectively stopped their proliferation.

These new cell lines represent valuable tools for studying HGBL-DH and for the *in vitro* testing of candidate therapies targeting HGBL-DH. LB5848-LYMP is also suitable for similar experiments *in vivo*.

Keywords: High-grade double-hit lymphoma, cell lines, MYC, BCL2

Introduction

High-grade B-cell lymphomas characterized by two concurrent chromosomal rearrangements – one involving the *MYC* locus at band 8q24, and one involving in most cases the *BCL2* locus at band 18q21 – are called double-hit high-grade B-cell lymphomas (HGBL-DH) [1]. In many HGBL-DH cases, the *MYC* and *BCL2* translocations bring these genes under the control of promoters or enhancers that, under normal circumstances, drive strong expression of the immunoglobulin (Ig) genes in B cells. As a result, the *MYC* and *BCL2* oncogenes are constitutively overexpressed in the malignant cells. MYC is a major transcriptional enhancer for genes involved in cell-cycle regulation, metabolism, ribosome biogenesis, protein synthesis and mitochondrial functions. It also represses genes involved in cell growth arrest and cell adhesion. On the other hand, *in vitro* MYC overexpression renders cells more sensitive to apoptosis under nutrient or growth-factor-deprivation conditions [2]. Upregulation of *MYC* should therefore lead to apoptosis, unless it is associated with additional anti-apoptotic alterations such as *TP53* mutations [3] or, as in HGBL-DH, BCL2 overexpression [4]. BCL2 is a protein of the outer membrane of the mitochondria that inhibits the pro-apoptotic proteins BAX and BAK, thereby prolonging cell survival [5]. Thus, in tumour cells the simultaneous overexpression of *BCL2* and *MYC* synergizes and leads to an aggressive malignant behaviour.

HGBL-DH are consistently highly aggressive lymphomas. As they invade the central nervous system more frequently than other B-cell lymphomas and are more resistant to conventional therapies, they result in a higher rate of primary resistance, relapse and mortality [6]. The 3-year overall survival rate of non-HGBL-DH patients following treatment with the standard R-CHOP regimen (rituximab, polychemotherapy and corticotherapy) is 75%, versus 46% for HGBL-DH patients [7].

In a minority of HGBL-DH, the second translocation involves the *BCL6* rather than the *BCL2* locus. BCL6 is a major transcriptional regulator of B-cell activation and selection during the germinal centre reaction. When overexpressed, BCL6 protects germinal center B-cells against DNA damage-induced apoptosis, notably via p53 repression [8]. In rare cases, *MYC*, *BCL2* and *BCL6* translocations are found concurrently in the so-called triple-hit HGBL [1].

Novel treatment strategies include intensified chemotherapy, e.g. addition of etoposide, autologous stem-cell transplantation, anti-CD19 chimeric antigen receptor T-cells, and bispecific T-cell engager antibodies [9–11]. There is an obvious need for new drugs that target the biological specificities of HGBL-DH. Inhibitors of the BCL2 family are currently being tested in clinical trials, with some preliminary success. Navitoclax (ABT-263) is an analogue of BH3-only proteins, which are natural inhibitors of BCL2. It has a high affinity for both BCL-2 and BCL-X_L. Venetoclax (ABT-199) is a selective BCL-2 inhibitor that avoids the thrombocytopenia caused by BCL-X_L inhibition [12, 13]. In addition, drugs that inhibit the bromodomain and extraterminal (BET) family of bromodomain proteins, which regulate MYC expression, are under development [14].

Several HGBL-DH cell lines have been described (reviewed in [15]). They are helpful tools to study the biology of HGBL-DH and to test experimental drugs. Here we report on the establishment and molecular characterization of two new HGBL-DH cell lines.

Material and methods

Cell culture

Resected tumour fragments were disrupted mechanically, washed in phosphate-buffered saline and resuspended at 1 x 10^6 cells/ml (24-well plate, 1 well) in RPMI 1640 (Gibco) supplemented with 10% fetal bovine serum (Gibco), L-arginine (0,55 mM), L-asparagine (0,24 mM), L-glutamine (1,5 mM), penicillin (100 U/ml) and streptomycin (0,1 mg/ml), hereafter referred to as complete medium. Cultures were maintained at 37°C in a humidified incubator with a 5% CO_2 atmosphere. The medium was changed every week.

Cell surface marker analysis

Immunophenotyping was performed on a calibrated 3-laser Navios flow cytometer (Beckman Coulter). Cell suspensions from disrupted tumour fragments or established cell lines were incubated with panels of monoclonal antibodies including those specific for CD3, CD4, CD5, CD10, CD19, CD22, CD38, CD40, CD43, CD44 (Beckman Coulter), CD8, CD11c, CD20, CD23, CD200 (Becton Dickinson), CD79a (Serotec) and surface kappa and lambda chains (Dako).

After incubation with the antibodies, cells were washed, resuspended in Isoton (Beckman Coulter) and a viability marker (7-aminoactinomycin D) was added to each cell suspension. The CXP 2.2 software (Beckman Coulter) was used for acquisition and analysis purposes.

Cytogenetic analysis

Karyotyping was performed on fragments of the tumoural lymph nodes according to standard procedures. Karyotypes and genomic alterations were reported according to the 2016 International System for Human Cytogenetic Nomenclature [16]. Dual-color fluorescence *in situ* hybridization (FISH) was performed on fixed nuclei and metaphases as reported

previously [17]. Commercially available probes were obtained from Abbott Molecular and Kreatech. All hybridized metaphases were captured on a Zeiss Axioplan 2 microscope and analyzed with the Isis software (Metasystems). Interphase FISH was performed in all cases and was complemented on cell lines with metaphase FISH (100-200 nuclei per sample).

Nucleic acid extraction

RNA and genomic DNA were purified with the RNA NucleoSpin Kit in combination with the RNA/DNA Buffer Set Kit (Macherey-Nagel). cDNA was obtained from RNA by reverse transcription with MMLV-RT (Invitrogen) and amplified by polymerase-chain reaction (PCR). *ACTB* and *GAPDH* PCR were performed as control for RNA and reverse transcription quality.

Confirmation of the common origin of each tumour and cell line pair.

DNA fingerprinting using the PowerPlex 16 HS System (Promega) was performed according to the manufacturer's instructions.

Detection of Epstein-Barr virus (EBV) DNA by PCR

PCR amplification of EBV genetic sequences was performed on genomic DNA extracted from the established cell lines using published primers and PCR conditions [18].

Cell cycle analysis

One million cells were harvested, washed in PBS, fixed in ethanol 70% and kept overnight at -20°C. Fixed cells were stained with 50 µg/ml propidium iodide (PI) at room temperature during 15 minutes. Flow cytometry analysis was performed on a LSRFortessa (Becton Dickinson) at low flow rate. Cell doublets were eliminated for data analysis.

Identification of rearranged VDJ immunoglobulin genes

The rearranged immunoglobulin heavy and light chain genes expressed in the tumour samples and cell lines were amplified by PCR on cDNA. In addition, for all Ig genes except *IGL*, a second PCR with internal primers was carried out on a 1:100 dilution of the first PCR product (see primers and PCR conditions in additional file 1). PCR products were sequenced and submitted to the IMGT database for identification [19]. Three malignant B-lineage cell lines, LB 1696-MYEL (a locally established myeloma cell line), DAUDI and EJM, and PBMCs from a healthy donor were used as controls for *IGA, IGD* + *IGM, IGG*, and *IGK* + *IGL* gene expression, respectively.

Xeno-transplantation in immunodeficient mice

NOD scid gamma (NSG) mice (Jackson Laboratory) were bred at the local animal facility. Cultured cells (LB5848-LYMP or LB5871-LYMP) were injected either intraperitoneally (up to 15 x 10^6 cells) or intravenously (up to 1 x 10^6 cells) into female mice.

Measurement of cell proliferation after treatment with a BCL2 inhibitor

Cultured cells (1.5 x 10^4 cells in 100 µl complete medium) were seeded in triplicate in 96-well flat-bottom cell culture plates. The BCL2 inhibitor ABT-199 (Selleckchem) was added at concentrations ranging from 6.4 nM to 20,000 nM. Cells were incubated in a humidified incubator with 5% CO_2. After 48h, 20 µCi of [methyl-^{3}H]-thymidine were added. Cells were lysed 24h later. DNA was transferred to 96-well UniFilter GF/C plates (PerkinElmer) with a cell harvester FilterMate 196 (Packard Bioscience) and 30 µl of MicroScint-O solution (PerkinElmer) were added to the filter. The incorporation of tritiated thymidine was measured with a Top Count NXT (PerkinElmer) microplate scintillation counter (PerkinElmer). The

values were normalized with the incorporation of tritiated thymidine in non-treated cells set to 100%.

Measurement of apoptotic and necrotic cells by flow cytometry

Apoptotic cells were detected by labelling with an anti-annexin V antibody coupled to APC (BioLegend), and propidium iodide (Sigma) staining of the cells. Acquisition was performed on a LSRFortessa (Becton Dickinson).

Western blot analysis

Dry cell pellets were resuspended in RIPA buffer (ThermoFisher Scientific) supplemented with Halt Protease and Phosphatase Inhibitors Cocktail (ThermoFisher Scientific). The amount of proteins was quantified by the BCA Protein Assay (Pierce, ThermoFisher Scientific). 20 µg of proteins were separated on NuPAGE 4-12% gels and transferred on nitrocellulose membranes using the iBlot device (Invitrogen). Binding of the anti-BCL2 (sc-7382, Santa Cruz) and anti-tubulin (#3873, Cell Signaling Technology) antibodies was carried out according to the manufacturer's instructions and revealed by chemiluminescence (SuperSignal, Pierce).

Targeted sequencing of 36 genes recurrently mutated in diffuse large B-cell lymphoma

40 ng of genomic DNA were used for library construction with the QIAseq 96-Index set B and a QIAseq targeted DNA Custom panel (Qiagen). The panel is based on the Lymphoma Study Association (LYSA) lymphopanel [20], and updated according to LYSA recommendations to include 36 genes (listed in additional file 2). Amplified libraries were sequenced on a MiSeq sequencer (Illumina). Alignment and variant calling were performed with the Biomedical Genomics Workbench software version 5.0.1 (Qiagen,

https://www.qiagenbioinformatics.com/). Annotations and variant analyses were performed using Highlander 14.10.3, a software that integrates 6 different variant prediction tools (http://sites.uclouvain.be/highlander/). A variant is considered as damaging if it is predicted as such by at least 4 of these tools.

Ethics approval and consent to participate

Anonymized human body material was obtained after patient consent and under approval of the Commission d'Ethique Biomédicale Hospitalo-Facultaire, Brussels, Belgium (reference 2014/28OCT/529).

Results

Case 1

A 75-year-old male patient was diagnosed with diffuse large B-cell lymphoma (DLBCL) of the germinal centre B-like (GCB) subtype by morphological analysis of a biopsied parotid lymph node (Figure 1A). The tumour stage was IB and the patient's age-adjusted international prognostic index (IPI) was 0. The tumour showed an abnormal hyperdiploid and complex karyotype including a t(14;18)(q32;q21) chromosomal translocation with duplication of the der(14)t(14;18)(q32;q21) and a high number of unidentified marker chromosomes and double minutes (Table 1). Fluorescence *in situ* hybridization (FISH) detected a *MYC* rearrangement at 8q24, associated with a high level amplification of the centromeric *MYC* probe within double minutes, as well as a *BCL2* rearrangement at 18q21 (Figure 1B-C). The *MYC* rearrangement was cryptic at the cytogenetic level. These results indicate a high-grade lymphoma with *MYC* and *BCL2* rearrangements according to the last 2017 WHO classification [1].

A fragment of the biopsied lymph node was disrupted mechanically, and the resulting cell population was put in culture. Small clusters of non-adherent cells became visible after a few weeks, and after 7 weeks a continuously dividing cell line with a doubling time of 54h was obtained. Additional file 3 shows its cell cycle profile. The cell line, named LB5848-LYMP, has been kept in culture for more than 15 months and has sustained repeated freezing and thawing. As shown in figure 1A, the morphology of the cultured cells was consistent with that of DLBCL cells. Both the cultured cells and the original tumour displayed the same surface markers, consistent with a B-cell malignancy, as assessed by flow cytometry (Table 2). FISH analysis showed a high level *MYC* amplification on double minutes and an unbalanced translocation of *BCL2* consistent with the abnormalities observed in the original tumour

(Figure 1B-C). The duplicated rearranged *BCL2* signals in the cell line suggest a clonal evolution from the original tumour.

DNA fingerprinting with 16 short tandem repeat markers confirmed that the LB5848-LYMP cell line originated from patient 1 (additional file 4). To exclude that the cell line derived from Epstein-Barr virus (EBV) transformed B-lymphocytes, we performed polymerase chain reaction (PCR) amplification of EBV genomic sequences: DNA from LB5848-LYMP was negative, whereas DNA from control B-lymphoblastoid cell lines was positive (additional File 5).

The LB5848-LYMP cells do not express surface Ig light chains (Table 2). We used RT-PCR and Sanger sequencing to characterize the rearranged Ig genes expressed by these cells. We identified a single *IGK* variable region sequence with 57.2% identity to the *IGKV1-17*02F* gene but with important nucleotide deletions and insertions causing an early frameshift. No fused *IGKJ* or *IGKC* genes were identified. The same truncated *IGKV1-17*02F* sequence was identified as a dominant sequence in the original tumour. No heavy chain gene product could be amplified from the cell line.

To assess their tumourigenic potential, we injected 1, 2 or 5 x 10^6 LB5848-LYMP cells intraperitoneally into immunodeficient NOD scid gamma (NSG) mice (1 mouse for each dose level). Abdominal tumours grew in the two mice injected with the highest doses (additional File 6). They were resected, dissociated and put in culture. The resulting proliferating cells were morphologically similar to the LB5848-LYMP cells and expressed the same *IGKV1-17*02F* sequence.

Case 2

A 64-year-old female patient with a history of breast cancer was diagnosed with follicular low-grade lymphoma in 2013. In April 2016, a biopsy from a cervical lymph node revealed a DLBCL of the GCB type (Figure 2A). The tumour stage was IIIA and the patient's age-adjusted IPI score was 1/3. The tumour exhibited an abnormal hyperdiploid and complex karyotype including a t(14;18)(q32;q21) translocation, several other chromosomal rearrangements and unidentified marker chromosomes (Table 1). FISH experiments detected chromosomal rearrangements of the *BCL2* and *MYC* loci, the latter being cryptic at the cytogenetic level (Figure 2 B-C). These observations establish a diagnosis of HGBL-DH.

Mechanically dissociated cells from the excised tumour were put in culture. After 6 weeks, continuous proliferation of cells was observed (with a doubling time of 62h). Additional file 3 shows its cell cycle profile. Since then, the cells have sustained repeated freezing and thawing. The cell line was named LB5871-LYMP. It formed single-cell suspensions in culture with morphological features of DLBCL (Figure 2A). Flow cytometry analysis showed that LB5871-LYMP cells had the same phenotype as the original tumour cells (Table 2). FISH analysis confirmed the presence of both *MYC* and *BCL2* rearrangements (Figure 2B-C). DNA fingerprinting confirmed that LB5871-LYMP cells derived from patient 2 (additional file 4). We excluded that LB5871-LYMP derived from EBV-transformed B cells by a negative PCR for EBV DNA (additional file 5).

Using RT-PCR amplification and sequencing, we identified the *IGHV3-15*01-IGHD2-2*01F-IGHJ6*03F IGG* and *IGKV1D-39*01F-IGKJ5*01F* Ig gene rearrangements. These rearrangements were dominant in the tumour and unique in the cell line.

LB5871-LYMP cells injected intraperitoneally (up to 15 x 10^6 cells) or intravenously (up to 1 x 10^6 cells) in NSG mice failed to give rise to detectable tumours.

Mutations in DLBCL-associated genes

Targeted high-throughput DNA sequencing of 36 selected genes recurrently mutated in DLBCL (listed in additional file 2) was performed on DNA extracted from the two cell lines. The observed non-synonymous mutations that are predicted to result in functional alteration of the protein ("damaging mutations") are displayed in table 3.

Both cell lines displayed bi-allelic inactivation of *TP53*. In both karyotypes, the first allele is lost with the deleted chromosome 17 (Table 1). The second allele carries an inactivating mutation. In LB5848-LYMP, the c.166G>T mutation introduces a premature stop codon and results in a truncated p53 protein. In LB5871-LYMP, the cysteine residue that is replaced by an arginine as a result of the c.526T>C mutation is required for p53 function, as previously demonstrated experimentally [21]. *BCL2* mutations were observed in LB5848-LYMP. Such mutations are reported to be associated with *BCL2* translocations in DLBCL [22]. LB5871-LYMP also displayed alterations in chromatin modifier genes (*ARID1A*, *MEF2B* and *EP300)* and in *TNFRSF14*.

In vitro sensitivity of the cell lines to a BCL2 inhibitor

We assessed whether the *in vitro* proliferation of LB5848-LYMP and LB5871-LYMP cells could be inhibited by ABT-199 (venetoclax), a selective BCL2 inhibitor currently investigated in patients with haematological malignancies overexpressing BCL2 [12]. Cells were incubated during 48h with increasing concentrations of ABT-199. Their proliferation rate was measured over 24h by ^{3}H-thymidine incorporation, and their death rate by flow

cytometry after combined annexin V and propidium iodide staining. A dose-dependent reduction of proliferation was observed for both cell lines (Figure 3A). We compared their sensitivity to ABT-199 to that of other lymphoma cell lines. SU-DHL-6, a known DH lymphoma cell line, and OCY-LY3, a *BCL2*-overexpressing DLBCL cell line, were both sensitive to ABT-199. In contrast, the drug had no or much less effect on RC-K8, a DLBCL cell line without *BCL2* overexpression, on two myeloid leukemia cell lines and on two B-lymphoblastoid cell lines. BCL2 protein levels, measured by Western blot in the same cell lines, were proportional to their sensitivity to ABT-199 (Figure 3B). ABT-199 induced dose-dependent cell death in LB5848-LYMP and LB5871-LYMP (Figure 3C).

Discussion

We report the establishment of two new human HGBL-DH cell lines. Both cell lines harbor *MYC* and *BCL2* rearrangements as confirmed by FISH analysis. In LB5848-LYMP cells, the *MYC* locus is also strongly amplified on double minutes. Both cell lines derive unambiguously from the respective primary HGBL-DH lesion, as indicated by similar morphologies, identical patterns of cell surface markers, identical DNA fingerprinting profiles and identical monoclonal immunoglobulin gene rearrangements. In the case of LB5871-LYMP, productive rearrangements at the heavy and kappa light chain loci lead to the production of an immunoglobulin detectable at the cell surface. In contrast, only a single truncated and unrearranged light chain gene is expressed in LB5848-LYMP, resulting in the absence of detectable surface immunoglobulin. Unproductive immunoglobulin rearrangement is a rare phenomenon that occurs in less than 5% of all DLBCL [23], but is more often observed in the GCB subtype [24], which corresponds to the subtype of LB5848-LYMP.

Beside *MYC* and *BCL2* rearrangements, both cell lines also showed bi-allelic inactivation of *TP53*, a characteristic feature of *MYC*/*BCL2* HGBL [25]. Of note, no mutation in *ID3* or *CCND3*, which belong to the molecular Burkitt signature also detected in a subset of HGBL, were observed [26].

LB5871-LYMP, the cell line derived from a transformed follicular lymphoma, exhibits a *TNFRSF14* mutation. Such mutations are observed in 40% of follicular lymphomas and are associated with worse prognosis [27, 28]. Three chromatin modifier genes (*ARID1A, MEF2B* and *EP300*) were also mutated in this cell line. These genes are classically mutated in follicular lymphomas [29] and in DLBCL [30].

HGBL-DH is a newly described, highly heterogeneous entity [1]. Our two biologically different HGBL-DH cell lines, LB5848-LYMP which is derived from a *de novo* lymphoma with mutations in *BCL2*, and LB5871-LYMP which is issued from a transformed follicular lymphoma with mutations in *TNFRSF14* and chromatin modifier genes, can be useful laboratory tools to study the biology of HGBL-DH, to identify potential therapeutic targets and to test new therapeutics *in vitro*. We tested the effect of the selective BCL2 inhibitor ABT-199 (venetoclax). In both cell lines proliferation was blocked in a dose-dependent manner. The sensitivity of LB5848-LYMP to the BH3-mimetic drug ABT-199 was not affected by its *BCL2* mutations, but these were located outside of the BH3 domain [31]. ABT-199 inhibition was also observed in other BCL2-overexpressing cell lines and correlated with BCL2 protein expression level. Our results support the further clinical development of BCL2 inhibitors in HGBL-DH patients.

Acknowledgements

We thank Aurélie Daumerie and Mélissa Vanhamme for excellent technical assistance.

Funding

MSD is a research fellow with Fonds National de la Recherche Scientifique (Belgium). This work was supported by grants from the Fondation Salus Sanguinis (Belgium) and the Fonds National de la Recherche Scientifique, Télévie under grant n°7.4668.15 (Belgium).

Declaration of interest statement

The authors declare that they have no competing interests.

Availability of data and material

The datasets used and/or analysed during the current study are available from the corresponding author on reasonable request.

References

1. Swerdlow SH, Campo E, Harris NL, Jaffe ES, Pileri SA, Stein H, et al. WHO Classification of Tumours of Haematopoietic and Lymphoid Tissues, Revised 4th Edition, Volume 2, Lyon: IARC;2017.

2. Dang C V., O'Donnell KA, Zeller KI, Nguyen T, Osthus RC, Li F. The c-Myc target gene network. Semin Cancer Biol. 2006;16:253–64.

3. Li S, Weiss VL, Wang XJ, Desai PA, Hu S, Cameron Yin C, et al. High-grade B-cell lymphoma with MYC rearrangement and without BCL2 and BCL6 rearrangements is associated with high P53 expression and a poor prognosis. Am J Surg Pathol. 2016;40:253–61.

4. Epperla N, Maddocks KJ, Salhab M, Chavez JC, Reddy N, Karmali R, et al. C-MYC–positive relapsed and refractory, diffuse large B-cell lymphoma: Impact of additional "hits" and outcomes with subsequent therapy. Cancer. 2017;123:4411–8.

5. Czabotar PE, Lessene G, Strasser A, Adams JM. Control of apoptosis by the BCL-2 protein family: implications for physiology and therapy. Nat Rev Mol Cell Biol. 2013;15:49–63.

6. Johnson NA, Slack GW, Savage KJ, Connors JM, Ben-Neriah S, Rogic S, et al. Concurrent expression of MYC and BCL2 in diffuse large B-cell lymphoma treated with rituximab plus cyclophosphamide, doxorubicin, vincristine, and prednisone. J Clin Oncol. 2012;30:3452–9.

7. Green TM, Young KH, Visco C, Xu-Monette ZY, Orazi A, Go RS, et al. Immunohistochemical Double-Hit Score Is a Strong Predictor of Outcome in Patients With Diffuse Large B-Cell Lymphoma Treated With Rituximab Plus Cyclophosphamide, Doxorubicin, Vincristine, and Prednisone. J Clin Oncol. 2012;30:3460–7.

8. Basso K, Dalla-Favera R. Roles of BCL6 in normal and transformed germinal center B cells. Immunol Rev. 2012;247:172–83.

9. Anderson MA, Tsui A, Wall M, Huang DCS, Roberts AW. Current challenges and novel treatment strategies in double hit lymphomas. Ther Adv Hematol. 2016;7:52–64.

10. Viardot A, Goebeler M-E, Hess G, Neumann S, Pfreundschuh M, Adrian N, et al. Phase 2 study of the bispecific T-cell engager (BiTE) antibody blinatumomab in relapsed/refractory diffuse large B-cell lymphoma. Blood. 2016;127:1410–6.

11. Locke FL, Neelapu SS, Bartlett NL, Siddiqi T, Chavez JC, Hosing CM, et al. Phase 1 Results of ZUMA-1: A Multicenter Study of KTE-C19 Anti-CD19 CAR T Cell Therapy in Refractory Aggressive Lymphoma. Mol Ther. 2017;25:285–95.

12. Souers AJ, Leverson JD, Boghaert ER, Ackler SL, Catron ND, Chen J, et al. ABT-199, a potent and selective BCL-2 inhibitor, achieves antitumour activity while sparing platelets. Nat Med. 2013;19:202–8.

13. Wilson WH, O'Connor OA, Czuczman MS, LaCasce AS, Gerecitano JF, Leonard JP, et al. Navitoclax, a targeted high-affinity inhibitor of BCL-2, in lymphoid malignancies: a phase 1 dose-escalation study of safety, pharmacokinetics, pharmacodynamics, and antitumour activity. Lancet Oncol. 2010;11:1149–59.

14. Trabucco SE, Gerstein RM, Evens AM, Bradner JE, Shultz LD, Greiner DL, et al. Inhibition of Bromodomain Proteins for the Treatment of Human Diffuse Large B-cell Lymphoma. Clin Cancer Res. 2015;21:113–22.

15. Drexler HG, Eberth S, Nagel S, MacLeod RAF. Malignant hematopoietic cell lines: in vitro models for double-hit B-cell lymphomas. Leuk Lymphoma. 2016;57:1015–20.

16. McGowan-Jordan J, Simons A, Schmid M. ISCN : an international system for human cytogenomic nomenclature (2016). Basel: Karger; 2016.

17. Duhoux FP, Ameye G, Lambot V, Herens C, Lambert F, Raynaud S, et al. Refinement of 1p36 alterations not involving PRDM16 in myeloid and lymphoid malignancies. PLoS One. 2011;6:1–9.

18. Ryan JL, Fan H, Glaser SL, Schichman SA, Raab-Traub N, Gulley ML. Epstein-Barr Virus Quantitation by Real-Time PCR Targeting Multiple Gene Segments. J Mol Diagnostics. 2004;6:378–85.

19. Giudicelli V, Brochet X, Lefranc M-P. IMGT/V-QUEST: IMGT standardized analysis of the immunoglobulin (IG) and T cell receptor (TR) nucleotide sequences. Cold Spring Harb Protoc. 2011;2011:695–715.

20. Dubois S, Viailly PJ, Mareschal S, Bohers E, Bertrand P, Ruminy P, et al. Next-generation sequencing in diffuse large B-cell lymphoma highlights molecular divergence and therapeutic opportunities: A LYSA study. Clin Cancer Res. 2016;22:2919–28.

21. Stoner CS, Pearson GD, Koç A, Merwin JR, Lopez NI, Merrill GF. Effect of Thioredoxin Deletion and p53 Cysteine Replacement on Human p53 Activity in Wild-Type and Thioredoxin Reductase Null Yeast. Biochemistry. 2009;48:9156–69.

22. Schuetz JM, Johnson NA, Morin RD, Scott DW, Tan K, Ben-Nierah S, et al. BCL2 mutations in diffuse large B-cell lymphoma. Leukemia. 2012;26:1383–90.

23. White, MT(ASCP) G, Zehnbauer, PhD, FACMG BA, Zutter, MD MM, Kaleem, MD Z. Lack of Expression of Surface Immunoglobulin Light Chains in B-Cell Non-Hodgkin Lymphomas. Am J Clin Pathol. 2000;113:399–405.

24. Evans AG, Spence JM, Spence SA, Rothberg PG, Burack R. Diffuse Large B-Cell Lymphoma Lacking Surface B-Cell Receptor Expression Are Germinal Center B- Cell (GCB) -Type and Lack Evidence of Known Downstream Activating Mutations. Blood. 2015;126:1453.

25. Gebauer N, Bernard V, Gebauer W, Thorns C, Feller AC, Merz H. TP53 mutations are frequent events in double-hit B-cell lymphomas with MYC and BCL2 but not MYC and BCL6 translocations. Leuk Lymphoma. 2015;56:179–85.

26. Bouska A, Bi C, Lone W, Zhang W, Kedwaii A, Heavican T, et al. Adult high-grade B-cell lymphoma with Burkitt lymphoma signature: Genomic features and potential therapeutic targets. Blood. 2017;130:1819–31.

27. Kotsiou E, Okosun J, Besley C, Iqbal S, Matthews J, Fitzgibbon J, et al. TNFRSF14 aberrations in follicular lymphoma increase clinically significant allogeneic T-cell responses. Blood. 2016;128:72–81.

28. Cheung K-JJ, Johnson NA, Affleck JG, Severson T, Steidl C, Ben-Neriah S, et al. Acquired TNFRSF14 mutations in follicular lymphoma are associated with worse prognosis. Cancer Res. 2010;70:9166–74.

29. Pastore A, Jurinovic V, Kridel R, Hoster E, Staiger AM, Szczepanowski M, et al. Integration of gene mutations in risk prognostication for patients receiving first-line immunochemotherapy for follicular lymphoma: A retrospective analysis of a prospective clinical trial and validation in a population-based registry. Lancet Oncol. 2015;16:1111–22.

30. Morin RD, Mendez-lago M, Mungall AJ, Goya R, Karen L, Corbett R, et al. Frequent

mutation of histone modifying genes in non-Hodgkin lymphoma. Nature. 2012;476:298–303.

31. Fresquet V, Rieger M, Carolis C, Garcia-Barchino MJ, Martinez-Climent JA. Acquired mutations in BCL2 family proteins conferring resistance to the BH3 mimetic ABT-199 in lymphoma. Blood. 2014;123:4111–9.

Figures legends

Figure 1. Cytology and FISH analysis of the tumour and the derived LB5848-LYMP cell line (case 1)

A. Morphology of the tumour cells (May-Grünwald-Giemsa staining).

B-C. FISH analysis of the *MYC* (B) and *BCL2* (C) loci with break-apart probes. Intact loci appear as fused red and green dots (dotted arrows). Separated red and green spots indicate chromosomal translocations (full arrows). In the case of *MYC*, the breakpoint is located in the blue probe, therefore the blue signal segregates with both the green and the red probes in case of translocation. FISH staining for *MYC* highlights the high-level amplification of the 5' centromeric probe on double minute chromosomes (green/blue signals). BCL2 FISH shows 2 red signals corresponding to a duplicated der(14)t(14;18)(q32;q21). The duplication of red and green signals in the cell line compared to the original tumour suggests a clonal evolution from the original tumour.

B-C Outer right. Position of the FISH probes on the corresponding loci.

Figure 2. Cytology and FISH analysis in the tumour and the derived LB5871-LYMP cell line (case 2)

A. Morphology of the tumour cells (May-Grünwald-Giemsa staining).

B-C. FISH analysis of the *MYC* (B) and *BCL2* (C) loci. Intact loci appear as fused red and green dots (dotted arrows). Separated red and green spots indicate chromosomal translocations (full arrows).

B-C Outer right. Position of the FISH probes on the corresponding loci.

Figure 3. Effect of BCL2 inhibition on the proliferation of the LB5848-LYMP and LB5871-LYMP cell lines

A. 1,5 x 10^4 cells of the indicated cell lines were treated with increasing concentrations of ABT-199 for 48h then incubated with 3H-thymidine. Tritiated thymidine uptake was measured after 24h. Values were normalized to the measured uptake of the corresponding untreated cell lines set to 100%. The results from the experiment are displayed in two panels (with LB5848-LYMP and LB5848-LYMP repeated) for the sake of clarity.

Left panel. LB5871-LYMP, LB5848-LYMP and SU-DHL-6 (double-hit lymphoma cell lines), OCI-LY-3 (BCL2-overexpressing DLBCL cell line), and RC-K8 (DLBCL cell line without BCL2 overexpression).

Right panel. LB5871-LYMP, LB5848-LYMP, HEL and TF-1 (myeloid leukemia cell lines) and LG-2-EBV and LB-2265-EBV (B-lymphoblastoid cell lines).

B. BCL2 and tubulin (control) protein expression in the cell lines from (A), assessed by Western blot.

C. LB5848-LYMP and LB5871-LYMP cell death was assessed by annexin V/propidium iodide co-staining and flow cytometry 48h after addition of increasing concentrations of the BCL2 inhibitor ABT-199.

Tables legends

Table 1. Karyotype formula of resected tumours

Table 2. Flow cytometry analysis of membrane markers on dissociated cells from the original tumour and on the derived cell line from cases 1 and 2

Table 3. Non-synonymous mutations in 36 recurrently mutated genes in DLBCL, detected by targeted DNA HTS-sequencing in the established cell lines. Only mutations with predicted functional alteration are reported.

Additional files legends

Additional file 1. Primers and PCR conditions for the identification of clonal VDJ immunoglobulin gene rearrangements

A mix of 6 forward primers binding to the conserved 5' extremity of the variable region genes was used (see below). Reverse primers are specific to the constant heavy or light chain genes.

Cycling conditions for the primary heavy chain PCR: 94°C 4 min, 30 cycles of [94°C 45 s, 50°C 45 s, 72°C 1 min 30 s + 2 s/cycle], 72°C for 10 min

Cycling conditions for the secondary heavy chain PCR: 94°C 4 min, 30 cycles of [94°C 45 s, 57°C 45 s, 72°C 45 s + 2 s/cycle], 72°C for 10 min

Cycling conditions for the primary light chain PCR: 94°C 4 min, 30 cycles of [94°C 1 min, 63°C 1 min, 72°C 1 min], 72°C for 10 min

Cycling conditions for the kappa secondary light chain PCR: 94°C 4 min, 30 cycles of [94°C 1 min, 65°C 1 min, 72°C 1 min], 72°C for 10 min

Additional file 2. List of genes included in the targeted DLBCL gene panel that were sequenced in the two cell lines

Additional file 3. Cell cycle profile of the cell lines assessed by propidium iodide (PI) staining and flow cytometry

Analysis revealed three distinct cell populations in LB5848-LYMP and LB5871-LYMP indicative of cells in the G0/G1, S and G2/M phases of the cell cycle.

Additional file 4. DNA fingerprinting analysis performed on the original tumours and the cell lines

Analysis of 16 short tandem repeat (STR) markers confirmed that each established cell line and its tumour counterpart derived from the same person. Discordant alleles are shown in bold and italic. They presumably arose from mutations that appeared during cell culture or represent PCR artifacts.

Additional file 5. Search for EBV DNA sequences by PCR on genomic DNA from the cell lines

PCR was performed on 50 ng genomic DNA. Established cell lines were shown to be negative for the two EBV-encoded BamH1 and EBNA1 genes. Two locally established B-lymphoblastoid cell lines (LB 3473-EBV and LB 3317-EBV) and the DLBCL RC-K8 cell line were used as positive and negative controls, respectively.

Additional file 6. LB5848-LYMP cells form tumour masses following injection into NSG mice

A. Abdominal tumours (white arrows) developed in an NSG mouse injected intraperitoneally with 5 x 10^6 LB5848-LYMP cells.

B. May-Grünwald-Giemsa staining of cultured cells derived from one tumour from (A).

FIGURE 1

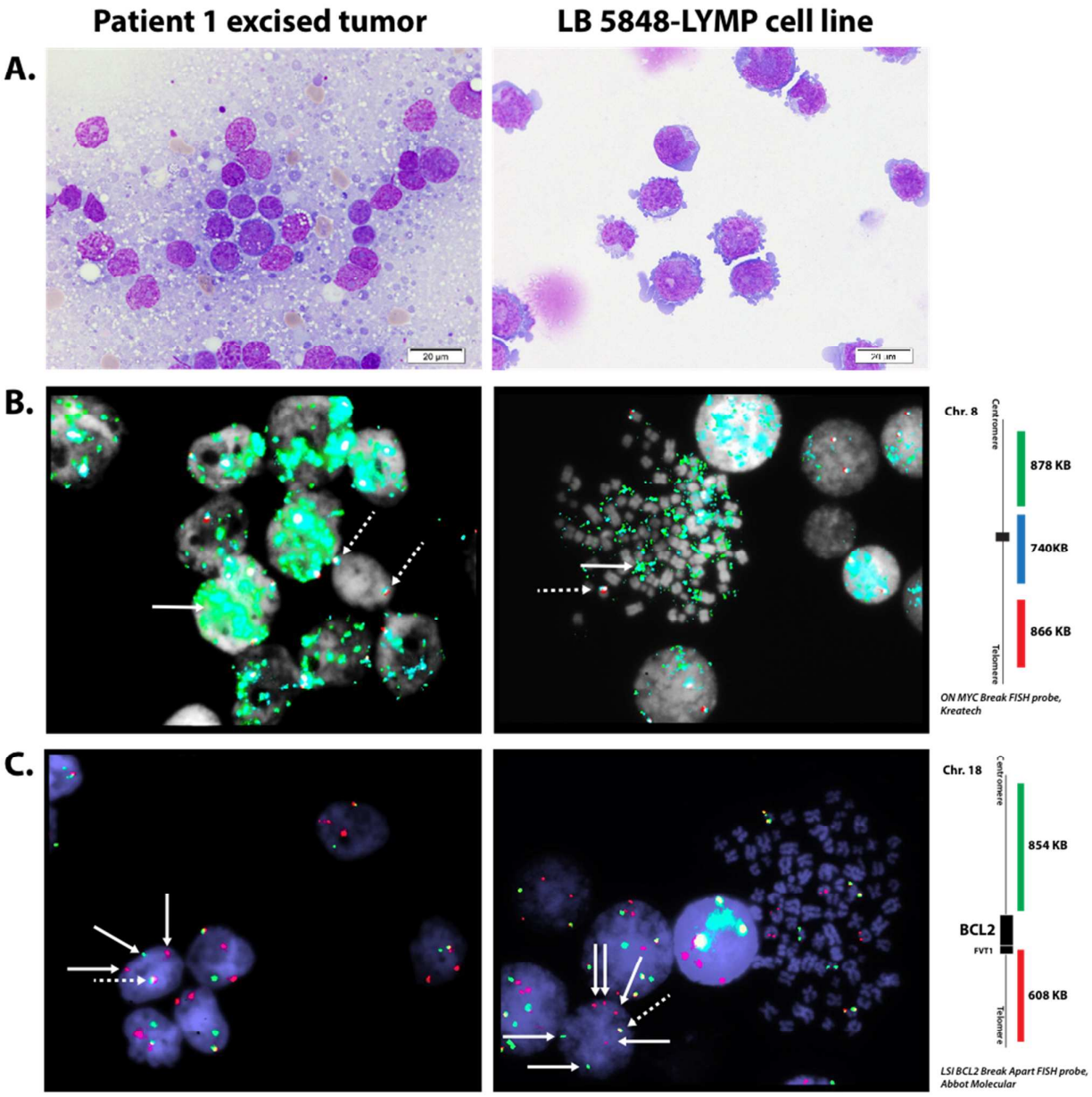
Patient 1 excised tumor
LB 5848-LYMP cell line
A.
20 µm
B.
Chr. 8
Centromere
878 KB
740KB
866 KB
Telomere
ON MYC Break FISH probe, Kreatech
C.
Chr. 18
Centromere
854 KB
BCL2
FVT1
608 KB
Telomere
LSI BCL2 Break Apart FISH probe, Abbot Molecular

Figure 2

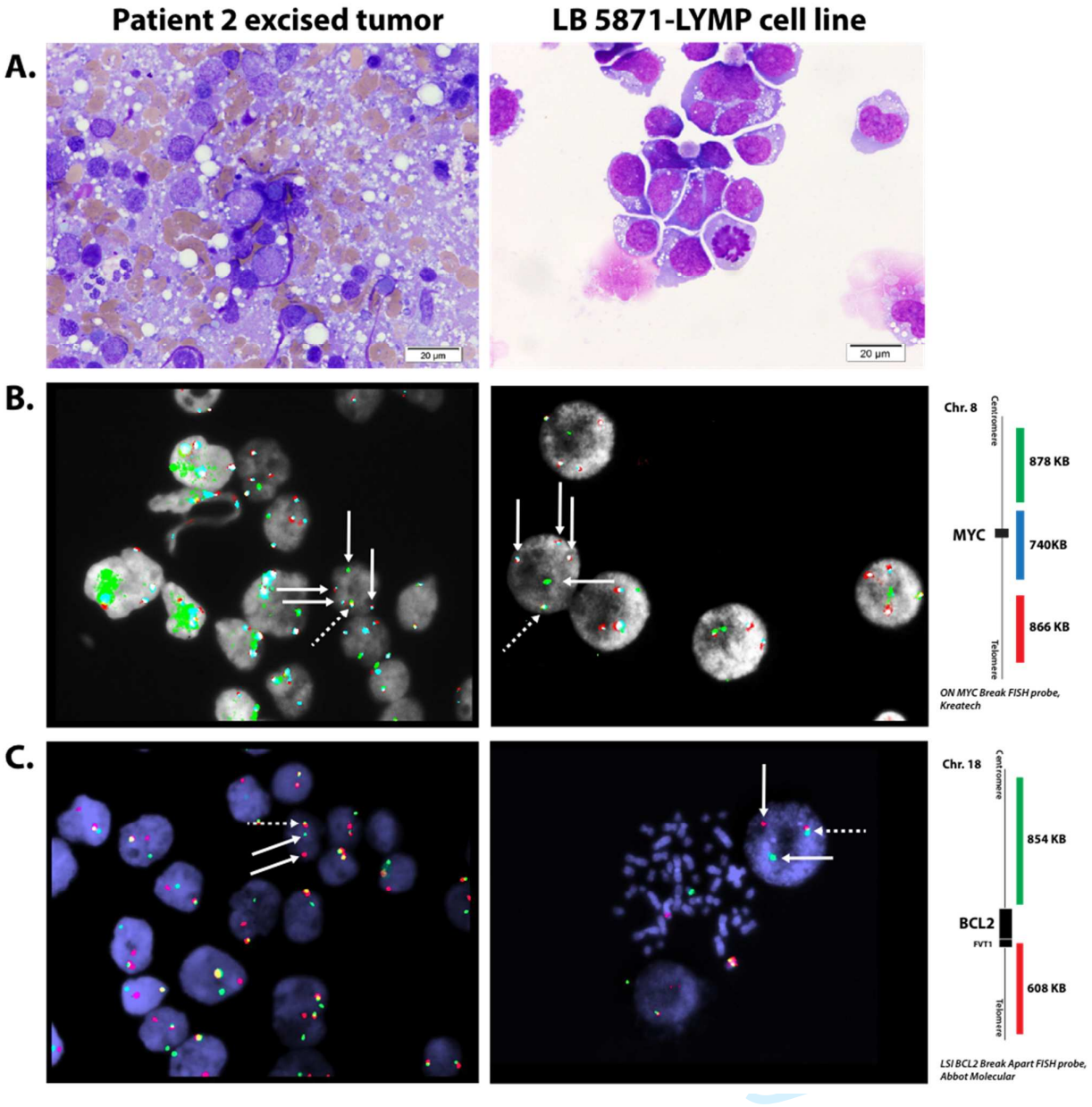
Patient 2 excised tumor
LB 5871-LYMP cell line
A.
20 µm
20 µm
B.
Chr. 8
Centromere
878 KB
MYC
740KB
866 KB
Telomere
ON MYC Break FISH probe, Kreatech
C.
Chr. 18
Centromere
854 KB
BCL2
FVT1
608 KB
Telomere
LSI BCL2 Break Apart FISH probe, Abbot Molecular

Figure 3

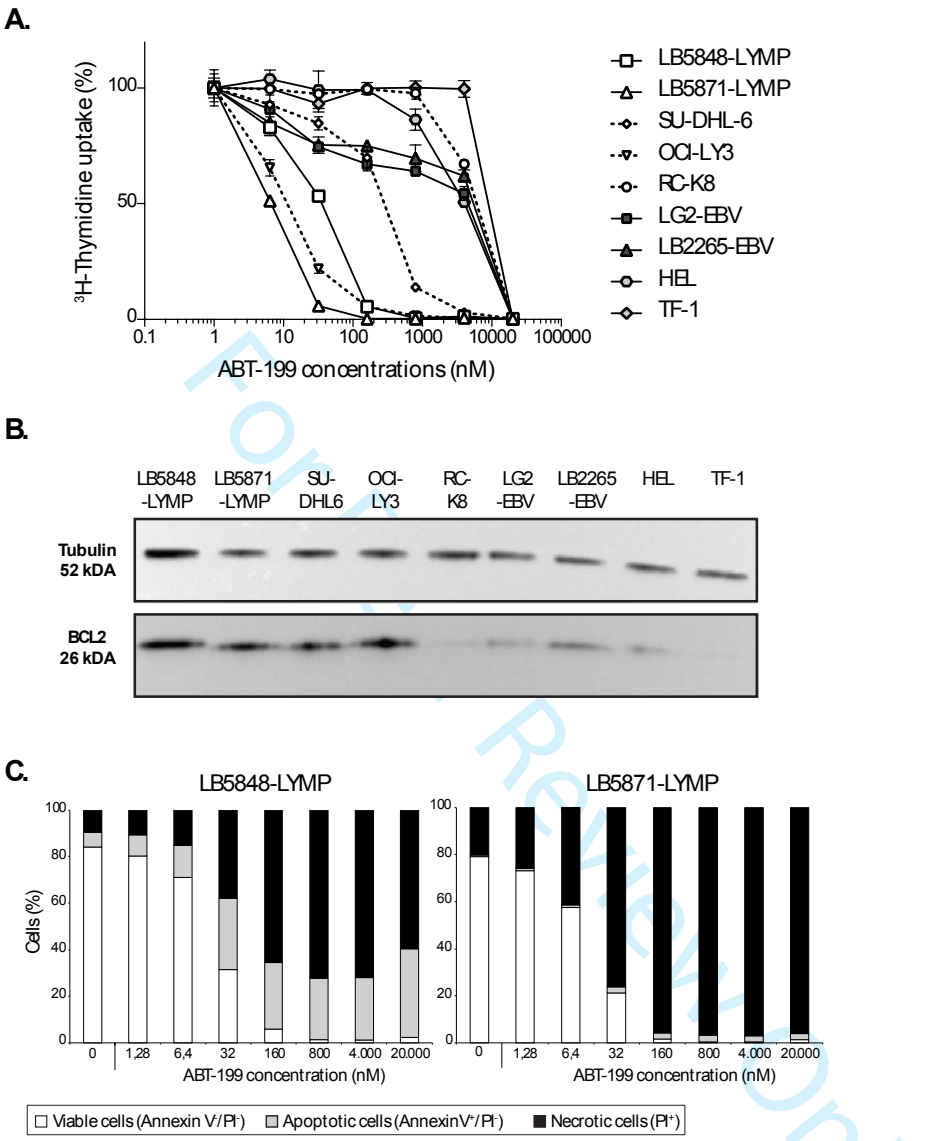

Table 1

Case 1: 48~50,X, -Y, -13,-13,t(14;18)(q32;q21),+der(14)t(14;18)(q32;q21),-17,add(17)(q21),-21, +mar1,+mar2,+mar3,+mar4,+mar5,+mar6,+mar7,+mar8,20~100dmin[8]/ 48~49,idem,-3,-6,+12[12]/ 46,XY[2]
Case 2: 45~48, -X, -2del(2)(p?13), -3, -6, -10, -13, -14,t(14;18)(q32;q21), -17,+mar1,+mar2,+mar 3,+mar4,+mar5,+mar6[2]/ 46~49,idem,add(6)(q2?1),-der(14)t(14;18)(q32;q21),der(18)t(14;18)(q32;q21)[4]/ 45~49,idem, add(6)(q2?1),-der(14)t(14;18)(q32;q21),der(18)t(14;18)(q32;q21),- 19,+mar7[7]/ 46~47,idem,add(1)(p36.?),add(6)(q2?1), -der(14)t(14;18)(q32;q21),der(18)t(14;18)(q32;q 21) -19,+mar7[3]/ 44~47,idem,add(6)(q2?1), -der(14)t(14;18)(q32;q21),der(18)t(14;18)(q32;q21),+mar8[3]/ 44~47,idem,add(6)(q2?1),-der(14)t(14;18)(q32;q21),der(18)t(14;18)(q32;q21),der(19)t(1; 19)(q21;q13.1-1)[3]

Table 2

Surface markers	Case 1		Case 2	
	Resected tumor	LB5848-LYMP cell line	Resected tumor	LB5871-LYMP cell line
CD5	-	-	-	-
CD10	+	+	-	+/-
CD19	+	+	+	+
CD20	+	+	+	+
CD79a	-	-	+/-	+
CD23	-	-	-	-
CD43	+	+	-	-
CD44	-	-	+/-	+
CD11c	-	-	-	-
CD200	-	-	-	-
CD22	+/-	+	+	+
CD3	-	-	-	-
CD4	-	-	-	-
CD8	-	-	-	-
CD38	+	+	+/-	+
CD40	+	+	+	+
Kappa light chain	-	-	+	+
Lambda light chain	-	-	-	-

Table 3

A. LB5848-LYMP

Chr. band	Gene	Genetic variant	Variant status	Variant allele frequency (%)	Variant site (exon)	Amino acid change
17p13	*TP53*	c.166G>T	Hemizygous (LOH chr. 17)	99,61	4	p.Glu56*
18q21	*BCL2*	c.77G>C	Heterozygous	25,9	1	p.Arg26Thr
		c.98G>A	Heterozygous	51,85	1	p.Gly33Glu
		c.386G>A	Heterozygous	50,78	1	p.Arg129His

B. LB5871-LYMP

Chr. band	Gene	Genetic variant	Variant status	Variant allele frequency (%)	Variant site (exon)	Amino acid change
1p36	*TNFRSF14*	c.20G>A	Heterozygous	50,3	2	p.Trp7*
		c.578dup	Heterozygous	44,69	6	p.Ala194fs
1p36	*ARID1A*	c.6415_6424del CCCCCCTTCA	Heterozygous	51,1	20	p.Pro2139fs
17p13	*TP53*	c.526T>C	Hemizygous (LOH chr. 17)	99,9	5	p.Cys176Arg
19p13	*MEF2B*	c.248A>T	Heterozygous	56,33	5	p.Asp83Val
22q13	*EP300*	c.4399T>G	Heterozygous	39,19	27	p.Tyr1467Asp

Additional file 1

Mix of degenerate forward primers binding to the leader region of the heavy chain variable region genes – primary PCR	
5'-TCACCATggACTgSACCTggA-3'	5'-CCATggACACACTTTgYTCCAC-3'
5'-TCACCATggAgTTTgggCTgAgC-3'	5'-AgAACATgAAACAYCTgTggTTCTT-3'
5'-ATggggTCAACCgCCATCCT-3'	5'-ACAATgTCTgTCTCCTTCCTCAT-3'

Mix of degenerate forward primers binding to the FRW1 region of the heavy chain variable region genes – secondary PCR	
5'-CAggTSCAgCTggTRCAgTC-3'	5'-CAgRTCACCTTgAAggAgTC-3'
5'-SAggTgCAgCTggTggAgTC-3'	5'-CAggTgCAgCTgCAggAgTC-3'
5'-gARgTgCAgCTggTgCAgTC-3'	5'-CAggTACAgCTgCAgCAgTC-3'

Reverse primer binding to IGHAC – primary PCR		**IgA – secondary PCR**	
Reverse	5'-TgggATTCgTgTAgTgCTTC-3'	Reverse	5'-gCATgTCACggACTTgCC-3'
IgD – primary PCR		**IgD – secondary PCR**	
Reverse	5'-AgggCTgTTATCCTTTgggT-3'	Reverse	5'-CTgATATgATggggAAC-3'
IgG – primary PCR		**IgG – secondary PCR**	
Reverse	5'-CgCTgCTgAgggAgTAgAgT-3'	Reverse	5'-AgTTCCACgACACCgTCAC-3'
IgM – primary PCR		**IgM – secondary PCR**	
Reverse	5'-TCTCAggACTgATgggAAgC-3'	Reverse	5'-gAAgCCCCgggTACTgCT-3'

Mix of forward primers binding to the kappa light chain variable regions	
5'-CTCTTCCTCCTGCTACTCTGGCTCCCAG-3'	5'-ATTTCTCTGTTGCTCTGGATCTCTG-3'
5'-CTGGGGCTGCTAATGCTCTGG-3'	5'-CAGCTTCCTCCTCCTTTGGATCTCTG-3'
5'-GGGTTTCTGCTGCTCTGGGTTCC-3'	5'-ATGAGGSTCCCYGCTCAGCTCCTGG-3'

Ig kappa – primary PCR		**Ig kappa – secondary PCR**	
Reverse	5'-gTTTCTCgTAgTCTgCTTTgCTCA-3'	Reverse	5'-gTgCTgTCCTTgCTgTCCTgCT-3'

Mix of forward primers binding to the lambda light chain variable regions	
5'-GGT CCT GGG CCC AGT CTG TGC TG-3'	5'-GGT CCT GGG CCC AGT CTG CCC TG-3'
5'-GCT CTG TGA CCT CCT ATG AGC TG-3'	5'-GGT CTC TCT CSC AGC YTG TGC TG-3'
5'-GTT CTT GGG CCA ATT TTA TGC TG-3'	5'-GGT CCA ATT CYC AGG CTG TGG TG-3'
5'-GAG TGG ATT CTC AGA CTG TGG TG-3'	
Ig lambda	
Reverse	5'-CAC CAG TGT GGC CTT GTT GGC TTG-3'

Additional file 2

chr1	chr2	chr3	chr6	chr7	chr8	chr9	chr12
ARID1A	*CXCR4*	*MYD88*	*CCND3*	*BRAF*	*MYC*	*NOTCH1*	*STAT6*
CD58	*XPO1*		*IRF4*	*CARD11*		*CDKN2A*	
ID3			*PIM1*	*EZH2*		*CDKN2B*	
NOTCH2			*PRDM1*				
TNFRSF14			*TNFAIP3*				

chr13	chr15	chr16	chr17	chr18	chr19	chr22	chrX
FOXO1	*B2M*	*CIITA*	*CD79B*	*BCL2*	*CD79A*	*EP300*	*BTK*
		CREBBP	*GNA13*		*MEF2B*		
		PLCG2	*TP53*		*TCF3*		
		SOCS1					

Additional file 3

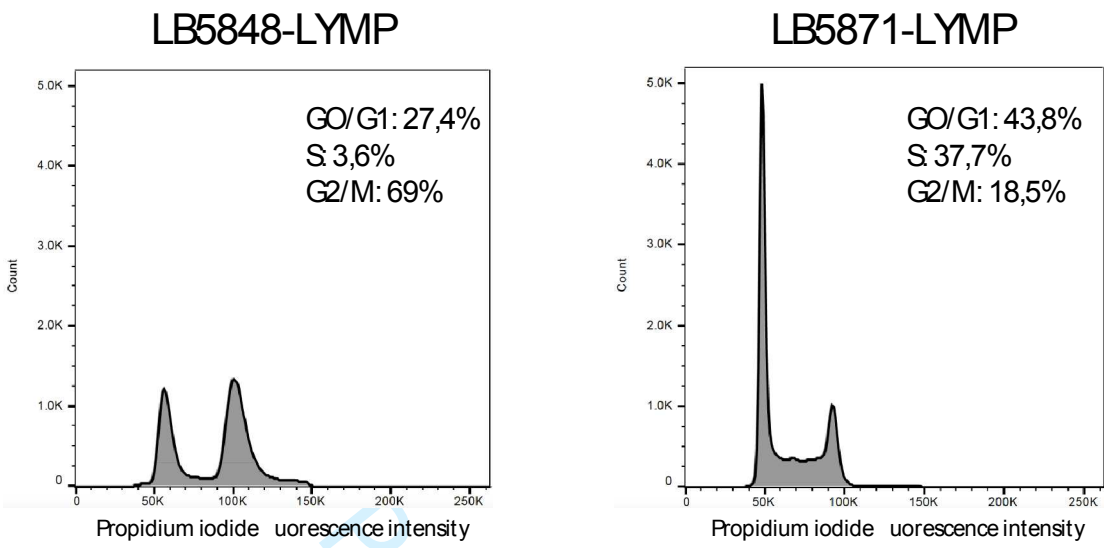

Additional file 4

STR marker	Tumor from case 1		LB-5848-LYMP		Tumor from case 2		LB-5871-LYMP	
	Allele 1	Allele 2	Allele 1	Allele 2	Allele 1	Allele 2	Allele 1	Allele 2
D3S1358	15		15		17		17	
TH01	8	9.3	8	9.3	7	9.3	7	9.3
D21S11	28	30	28	30	29	30	29	30
D18S51	17	22	17	22	12	16	12	16
Penta_E	10	11	10	11	7	11	7	11
D5S818	11	12	11	12	11	13	11	13
D13S317	10	12	10	12	11	13	11	13
D7S820	12		12		8	10	8	10
D16S539	11	12	11	12	9	11	9	11
CSF1PO	11	13	11	13	10	12	10	12
Penta_D	12	16	12	16	10		10	
AMEL	X		X		X		X	
vWA	17		17		14	15	14	15
D8S1179	13		13		8	13	8	13
TPOX	***8***	11	11		8		8	
FGA	20	25	20	25	22	***24***	22	***25***

Additional file 5

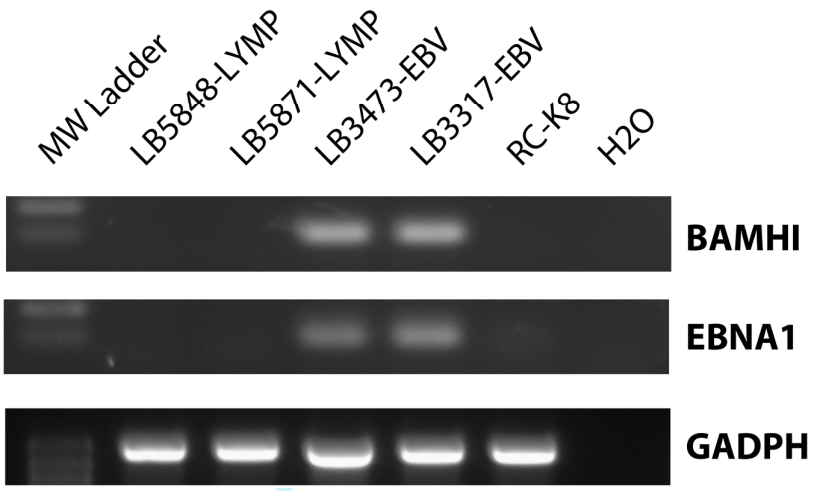

Additional file 6